Developmental Cell
Article

piggyBac-Based Mosaic Screen Identifies a Postmitotic Function for Cohesin in Regulating Developmental Axon Pruning

Oren Schuldiner,[1] Daniela Berdnik,[1] Jonathan Ma Levy,[1] Joy S. Wu,[1] David Luginbuhl,[1] Allison Camille Gontang,[1] and Liqun Luo[1,*]
[1]Howard Hughes Medical Institute, Department of Biological Sciences and Neurosciences Program, Stanford University, Stanford, CA 94305, USA
*Correspondence: lluo@stanford.edu
DOI 10.1016/j.devcel.2007.11.001

SUMMARY

Developmental axon pruning is widely used to refine neural circuits. We performed a mosaic screen to identify mutations affecting axon pruning of *Drosophila* mushroom body γ neurons. We constructed a modified *piggyBac* vector with improved mutagenicity and generated insertions in >2000 genes. We identified two cohesin subunits (*SMC1* and *SA*) as being essential for axon pruning. The cohesin complex maintains sister-chromatid cohesion during cell division in eukaryotes. However, we show that the pruning phenotype in $SMC1^{-/-}$ clones is rescued by expressing *SMC1* in neurons, revealing a postmitotic function. $SMC1^{-/-}$ clones exhibit reduced levels of the ecdysone receptor EcR-B1, a key regulator of axon pruning. The pruning phenotype is significantly suppressed by overexpressing EcR-B1 and is enhanced by a reduced dose of EcR, supporting a causal relationship. We also demonstrate a postmitotic role for SMC1 in dendrite targeting of olfactory projection neurons. We suggest that cohesin regulates diverse aspects of neuronal morphogenesis.

INTRODUCTION

Developmental axon pruning is widely used for the maturation and refinement of neural circuits (reviewed in Luo and O'Leary, 2005). In many well-documented cases, neurons first extend exuberant branches, and later prune away inappropriate branches with precise spatial and temporal control. Developmental axon pruning can occur by several distinct cellular mechanisms, including distal-to-proximal retraction (e.g., Liu et al., 2005; Portera-Cailliau et al., 2005); localized degeneration, in which defined segments of axons break into pieces that are taken up by surrounding cells (e.g., Watts et al., 2003, 2004; Awasaki and Ito, 2004; Portera-Cailliau et al., 2005); and "axosome shedding," in which distal ends of retracting axons are engulfed by nearby cells (Bishop et al., 2004). Developmental axon pruning, particularly that involving localized degeneration, also shares some molecular and mechanistic similarities with axon degeneration after nerve injury (Raff et al., 2002; Hoopfer et al., 2006).

Developmental axon pruning of mushroom body (MB) γ neurons in *Drosophila* occurs by localized degeneration (Watts et al., 2003) and is an appealing system for studying mechanisms of axon pruning. During metamorphosis, MB γ neurons prune their dendrites completely and prune axons to a specific branch point in a stereotypic manner (Lee et al., 1999). The initiation of pruning is regulated by the cell-autonomous action of the steroid hormone ecdysone receptor B1 (EcR-B1) and its coreceptor Ultraspiracle (Usp) (Lee et al., 2000a). For pruning to occur, γ neurons must also have a functional ubiquitin proteasome system (UPS) (Watts et al., 2003). Lastly, degenerated axon fragments are engulfed by glia (Awasaki and Ito, 2004; Watts et al., 2004). Similar molecular pathways appear to be used in other *Drosophila* neurons to direct developmental pruning of axons and dendrites during metamorphosis (Schubiger et al., 2003; Kuo et al., 2005; Marin et al., 2005; Williams and Truman, 2005). Despite the widespread use of these molecular pathways, our understanding of the underlying mechanisms is far from complete.

Forward genetic screens are a powerful and unbiased strategy for identifying molecules involved in complex biological processes. To study late developmental events and to identify genes that have pleiotropic functions, forward genetic screens in mosaic tissues (e.g., Xu and Rubin, 1993; Newsome et al., 2000a) have been developed. Furthermore, mosaic-labeling techniques such as the MARCM system (mosaic analysis with a repressible cell marker) (Lee and Luo, 1999) allow for visualization of only homozygous mutant cells, thereby further increasing the resolution of phenotype detection (e.g., Lee et al., 2000a). Compared to mutations induced by chemical mutagens such as EMS, transposon insertional mutagenesis permits rapid mapping of a causal mutation. However, P-element-based mutagenesis is not easily adapted to FLP/FRT-based mosaic screens. Recently, the *piggyBac* transposon has been shown to transpose effectively in *Drosophila* without destabilizing P elements (Hacker et al., 2003). We describe here a mosaic *piggyBac*-based insertional mutagenesis screen in *Drosophila* that identifies the cohesin complex as being required for axon pruning.

Cohesin is a highly conserved, multisubunit complex required for sister-chromatid cohesion during mitosis and meiosis. The cohesin complex is comprised of Smc1, Smc3, Scc1/Rad21, and Scc3/Stromalin (SA) (reviewed in Losada and Hirano, 2005; Nasmyth and Haering, 2005). Current data suggest a model in which Smc1, Smc3, and Rad21 form a ring that

embraces sister chromatids, whereas SA binds to Rad21 and probably has a regulatory function (Gruber et al., 2003; Huang et al., 2005; reviewed in Nasmyth, 2005; Hirano, 2006). Cohesin is loaded onto chromosomes with the assistance of another complex comprised of Scc2/Nipped-B and Scc4/Mau-2 (Ciosk et al., 2000; reviewed in Dorsett, 2007). The cohesin complex holds sister chromatids together until the onset of anaphase, when Rad21 is cleaved by Separase to enable their separation (Uhlmann et al., 2000; Jager et al., 2001).

Using a *piggyBac* mutator that is compatible with mosaic analysis and appears to efficiently disrupt genes even when inserted into introns, we have generated a large *piggyBac* mutant collection. Our screen in MB neurons revealed that mutations in *SMC1* and *SA*, two subunits of the cohesin complex, disrupt axon pruning and cause neuroblast-proliferation defects. Postmitotic expression of a wild-type (WT) *SMC1* transgene is sufficient to rescue axon-pruning phenotypes without rescuing the neuroblast-proliferation defects. We provide evidence that this postmitotic function of SMC1 is mediated through the regulation of EcR-B1 levels. SMC1 also regulates dendrite targeting in postmitotic olfactory projection neurons. Thus, in addition to its classic function in chromosome cohesion, our study indicates that the cohesin complex also plays an essential role in neurons to regulate their morphogenesis.

RESULTS

Insertional Mutagenesis with a Modified *piggyBac* Transposon

To increase mutagenicity of existing *piggyBac* elements and to specifically render the high proportion of intronic insertions mutagenic (Hacker et al., 2003), we added splice acceptors followed by stop codons in all three frames in both orientations of the mutator (Figure 1A). We also swapped the existing marker with a DsRed fluorescent protein to allow for live screening of brains with MARCM clones expressing GFP.

Mobilization of mutator elements was performed by using starter insertions on the X or second chromosomes (Supplemental Experimental Procedures, see the Supplemental Data available with this article online). All insertions occurred in a quadruple FRT background (FRTs 40A, G13, 2A, and 82B) such that nearly the entire second and third chromosomes can be subjected to mosaic screening. We developed a protocol to determine chromosomal insertion sites by inverse PCR from a single fly (Figure 1B; Supplemental Experimental Procedures). This has allowed us to map the insertion sites before a stable stock must be established and to discard insertions that were not successfully mapped (see below) or did not disrupt genes.

We sequenced 4867 insertions and mapped 4144 independent insertions, which are evenly distributed among all chromosome arms (Figure 1D). We failed to map insertions in repetitive regions, or those that yielded very short sequences. The distribution of the insertions with respect to the structure of genes is similar to what was previously reported (Hacker et al., 2003). Approximately 80% of mapped insertions were within transcriptional units, or up to 1 kb upstream of the predicted start of transcription (putative promoter). The remaining 20% were outside of these areas and were considered intergenic insertions (Figure 1D). Although intergenic insertions could potentially disrupt a distant enhancer or an unannotated gene, we discarded these insertions and those on the fourth chromosome or in centromeric regions, as they are not amenable to mosaic analysis. The largest fraction of insertions within transcriptional units was in introns (46%), justifying our effort to add splice traps to the mutator.

The 3241 independent intragenic insertions hit 2061 different genes, corresponding to ~15% of the annotated genes in the *Drosophila* genome (Celniker et al., 2002). The rate at which we target new genes indicates that the screen is far from reaching saturation (Figure 1C). A total of 69% of the genes were hit once, 3% were hit more than 4 times, and the most-hit gene was hit 13 times (Figure 1E). This distribution is consistent with the observations that *piggyBac* insertion is not random, but is less biased than P-element insertions (Bellen et al., 2004; Thibault et al., 2004).

Table S1 provides a comprehensive list of 1920 insertions targeting 1803 genes that are still available and can be obtained from the *Drosophila* Genetic Resource Center (DGRC), Kyoto, Japan (http://www.dgrc.kit.ac.jp/en/index.html). These can be used for any mosaic or nonmosaic forward screens or candidate mutant analyses.

Mutagenicity of *piggyBac* Insertions

To estimate the mutagenicity of our insertions, we determined the rate at which we generate homozygous lethal mutations. Our average rate is 28% (Figure 1F), which is higher than in previous studies (9%–22%) (Hacker et al., 2003; Thibault et al., 2004). Two factors likely contribute to this high lethality rate: the elimination of intergenic insertions and the addition of splice traps to the mutator. As expected, insertions in the 5′UTR and coding sequence (CDS) are most mutagenic (38% and 37% lethality, respectively), whereas insertions in the 3′UTR are the least mutagenic (13%). Intronic insertions are highly mutagenic (29% lethality), suggesting that the splice trap indeed improves mutagenicity. As only about one-third of the genes are expected to be essential for viability (Miklos and Rubin, 1996), this high lethality rate suggests that almost every insertion is mutagenic. A rate greater than the predicted one-third lethality rate in 5′UTR and CDS could be due to preferential insertions in active genes, as previously shown for P elements (Liao et al., 2000), genetic background (a result of having FRTs on four chromosome arms), or both. A total of 17% of our screened mutants showed abnormal MB phenotypes. When plotted alongside the lethality rate, we observe that the distributions are similar (Figure 1F), confirming that insertions in the 5′UTR, CDS, and introns likely create strong mutant alleles.

Another way to estimate the mutagenicity is to compare the defects caused by *piggyBac* insertions to phenotypes of known mutants in MB development by using MARCM analysis (see Experimental Procedures). The MB is comprised of three major types of neurons born sequentially from four neuroblasts in each hemisphere (Figure 2A). These neuronal types can be distinguished by their distinct projections and differential expression of Gal4 lines and FasII (Figures 2A and 2B) (Ito et al., 1997; Crittenden et al., 1998; Lee et al., 1999). Given the sequential birth and stereotypical projections, mutant phenotypes offer insights into the nature of the pathways affected. For example, MARCM neuroblast clones mutant in genes that affect

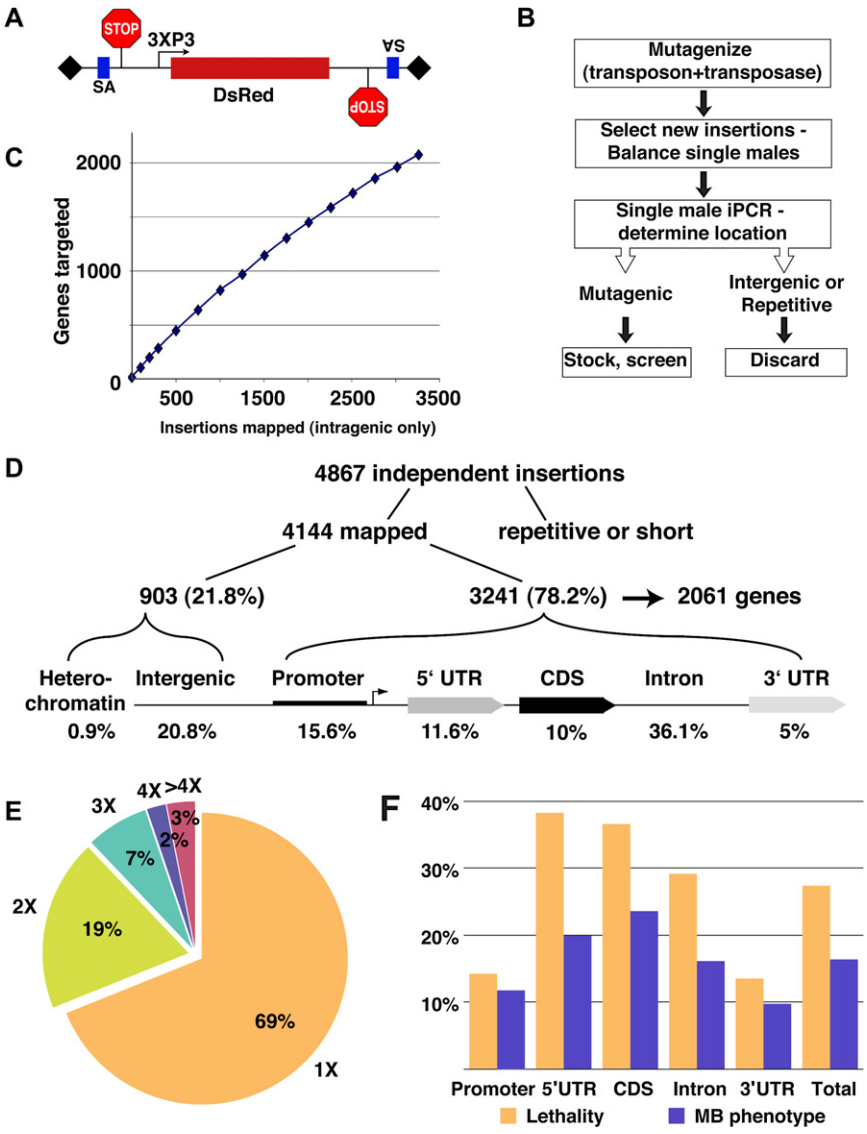

Figure 1. Overview of *piggyBac*-Based Insertional Mutagenesis

(A) Our modified *piggyBac* mutator element contains, in both orientations, a splice acceptor (SA) followed by stop codons in all three reading frames; it is marked with a DsRed reporter. 3XP3 is a synthetic promoter expressed mainly in the eye (Sheng et al., 1997) and was previously shown to effectively drive the expression of different fluorescent proteins as markers for *piggyBac* (Horn et al., 2000).

(B) Mutant generation scheme; see text and the Supplemental Experimental Procedures for details.

(C) Number of genes targeted plotted against intragenic insertions mapped.

(D) Distribution of *piggyBac* transposons with regard to a generic gene structure.

(E) Frequency distribution of 3241 independent insertions that fall within transcriptional units of 2061 different genes.

(F) Rates of lethality and MB mutant phenotype for insertions in different parts of the transcriptional unit.

proliferation should exhibit reduced cell numbers and should be comprised exclusively of the early-born γ neurons (Figures 2A and 2B). Neuroblast clones mutant in genes that affect neuronal survival should also have reduced cell numbers, but they should have both early- and late-born neurons.

MARCM analysis of insertions within three genes shows phenotypes very similar to previously reported mutants (Figures 2C–2E). (1) An intronic insertion in *Uba1* (Figure 2Ca) phenocopies a previously reported mutant (Watts et al., 2003). Compared with WT MB neuroblast clones (Figure 2Cb), mutation in *Uba1* results in a proliferation defect, as no late-born neurons appear in the mutant clone (asterisks in Figures 2Cc and 2Cd). In addition, some γ axons fail to prune (arrows and insets in Figures 2Cc and 2Cd), and they show signs of degeneration (arrowheads in Figures 2Cc and 2Cd). (2) Two intronic insertions in *twinstar* (*tsr*) inserted at the same site but in opposite orientation (Figure 2Da) result in an axon extension defect (asterisks in Figures 2Db–2Dd), as previously reported (Ng and Luo, 2004) (compare Figure 2Db to Figures 2Dc and 2Dd and to WT in Figure 2Ca). (3) An insertion in the 5′UTR of *trio* (Figure 2Ea) causes a proliferation defect of the neuroblast that lacks the last-born α/β neurons, a phenotype also observed with a previously characterized strong loss-of-function allele (Newsome et al., 2000b) (compare Figure 2Ec to Figure 2Ed and to WT in Figure 2Eb). These results confirm that our *piggyBac* insertions can create strong loss-of-function alleles.

To verify that the mutagenicity caused by intronic insertions is due to the splice trap, we performed RT-PCR experiments with appropriate primers for five different homozygous, viable insertions (Figure S1). Semiquantitative RT-PCR shows that in 5/5 cases we can detect the *piggyBac*-trapped transcript. Importantly, when comparing homozygous mutants to heterozygous flies, the endogenous transcripts were undetectable in 2/5 cases, reduced in another 2/5 cases, and exhibited no change in 1/5 cases. These data suggest that not all intronic insertions are equally mutagenic, consistent with our finding that the lethality rate of intronic insertions is lower compared with insertions in 5′UTRs or CDSs (Figure 1F).

Mutants Can Be Readily Screened by Using MARCM

Utilizing these *piggyBac* mutants, we have screened for defects in axon pruning of MB γ neurons. A salient advantage of performing transposon insertional mutagenesis is the ease of mapping the entire insertion collection, which allows for a genomic perspective for a particular phenotype. For example, while screening for mutations that affect axon pruning, we observed that the most common defect in MB development is a reduction in cell number comprising a neuroblast clone, most likely due to a proliferation defect.

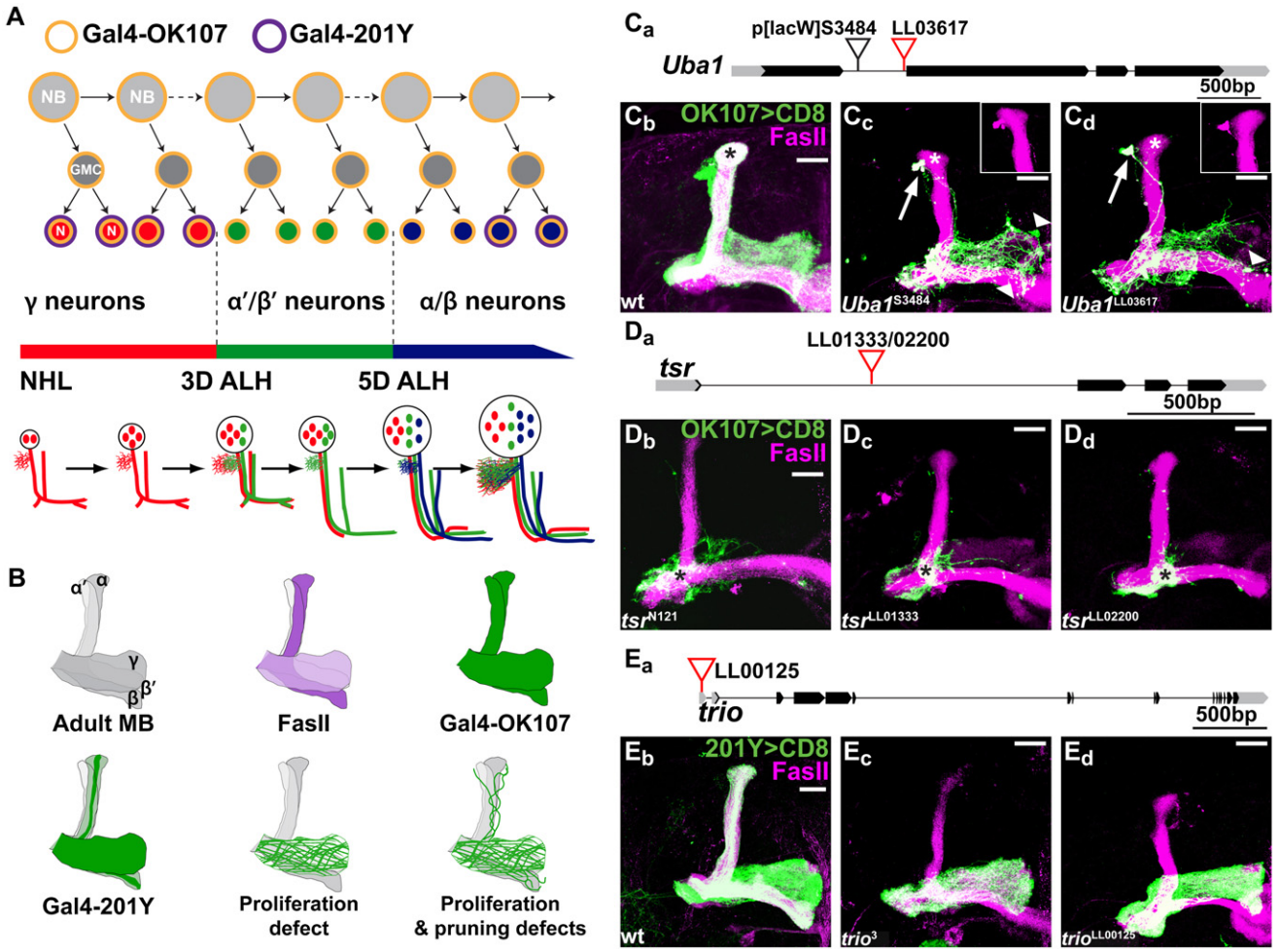

Figure 2. Phenotypic Comparison of *piggyBac* and Previously Characterized Alleles

(A) Scheme of sequential generation of MB neurons. MB neurons are generated from four neuroblasts (NBs) per hemisphere. Each NB divides asymmetrically to generate another NB and a ganglion mother cell (GMC), which divides once more to generate two postmitotic neurons (N). MB neuroblasts sequentially give rise to γ neurons (red), α′/β′ neurons (green), and α/β neurons (blue) according to the depicted developmental timeline. NHL, newly hatched larvae; 3D ALH, 3 days after larval hatching. Gal4-OK107 is expressed in all MB neurons, including dividing NBs (orange outline). Gal4-201Y is expressed in postmitotic γ neurons and in a subset of later-born α/β neurons (purple outline). A schematic representation of the stereotypical projection of MB neurons at different developmental stages is shown in the lower part of the panel. Adapted from Lee et al. (1999).

(B) The schematic drawings (from top left to bottom right) show: an adult MB with five axon lobes contributed by γ, α′/β′, and α/β neurons; that anti-FasII labels the γ lobe weakly and the α/β lobes strongly; Gal4-OK107 and Gal4-201Y expression patterns in the corresponding lobes; MB MARCM neuroblast clones defective in proliferation, with axons only innervating the γ lobe; and MB neuroblast clones defective in proliferation and pruning (as is the case for $Uba1^{-/-}$ and $SMC1^{-/-}$ clones), with residual unpruned γ axons around the dorsal lobes.

(C) (a) *piggyBac* line LL03617 is inserted in the first intron of *Uba1*. Compared to (b) WT MB clones, (d) homozygous $Uba^{LL03617}$ MB neuroblast clones in adults exhibit neuroblast-proliferation and axon-pruning defects, and signs of axon degeneration, similar to the previously reported phenotype of the (c) strong loss-of-function Uba^{S3484} (Watts et al., 2003). Arrows point to unpruned dorsal projections that are positive for FasII (insets). Arrowheads show blebbing and sparse axons; asterisks mark late-born α/β neurons.

(D) (a) *piggyBac* lines LL01333 and LL02200 are inserted in opposite orientations at the same location in the first intron of *twinstar* (*tsr*). (c and d) MB neuroblast clones homozygous for either insertion mostly contain axons that fail to extend beyond the branching point (asterisks), similar to the (b) axon growth phenotypes previously described for null mutation tsr^{N121} (asterisk) (Ng and Luo, 2004).

(E) (a) *piggyBac* line LL00125 is inserted in the 5′UTR of *trio*. (d) MB neuroblast clones homozygous for $trio^{LL00125}$ do not contain late-born α/β neurons, present in (b) WT neuroblast clones, indicating a neuroblast-proliferation defect. (c) This phenocopies a strong loss-of-function $trio^{3}$ mutant clones.

Black blocks, CDS; gray blocks, UTRs; lines, introns. All images in this and subsequent figures are confocal z-stacks of MB neurons and their axons, unless otherwise stated. The scale bars are 20 μm. Genotypes are described in Supplemental Data.

Table S2 provides the list of all *piggyBac* insertions that cause such defects. Figure S2 shows a few examples of insertions that affect clone size with different severity. As expected, genes essential for neuroblast proliferation are involved in housekeeping functions such as metabolism, transcription, translation, in addition to cell-cycle progression. For example, *Top2* is a topoisomerase essential for DNA replication, repair, and transcription; *SMC2* is a subunit of condensin important for chromosome

condensation; *polo* is a kinase involved in cell-cycle regulation; and *tws* is a protein phosphatase type 2A involved in the cell cycle. Hereafter, we focus on studies of the cohesin complex, identified in our screen to play a role in MB neuroblast proliferation as well as in γ neuron axon pruning.

SMC1 Is Required for Axon Pruning

In our screen, we identified an insertion in the third exon of *SMC1* (Figure 3E) that inhibits axon pruning in neuroblast clones (Figure 3). To follow the development of $SMC1^{-/-}$ γ neurons, we used Gal4-201Y, which is expressed in all γ and in a subset of late-pupal-born α/β neurons (see Figures 2A and 2B). We find that $SMC1^{-/-}$ γ neurons extend axons normally during larval development, as can be seen by their axonal extension into the dorsal and medial lobes at 0 hr after puparium formation (APF) (compare Figure 3Ca to Figure 3Ba; diagram in Figure 3A). However, when examined at the peak of pruning (18 hr APF) (Figure 3A), most WT γ neurons have completely pruned their axons within the dorsal and medial lobes (Lee et al., 1999; Watts et al., 2003), whereas $SMC1^{-/-}$ γ neurons retain many unpruned axons (compare Figure 3Cb to Figure 3Bb). Unpruned axons from $SMC1^{-/-}$ γ neurons persist in adult brains (compare Figure 3Cc to Figure 3Bc; schematized in Figure 2B). The dorsal axons in Figure 3Cc (arrows) can be distinguished as unpruned γ neurons, but not as α/β neurons (which are also labeled by Gal4-201Y), as they are outside the FasII fascicle (magenta) representing unlabeled, heterozygous α/β neurons derived from the other three MB neuroblasts.

In addition to the pruning defect, we observed that $SMC1^{-/-}$ neuroblast clones have fewer cells compared to WT clones (compare Figure 3Cc with Figure 3Bc and Figure 3Ca with Figure 3Ba) (the average clone size in WT and mutant at 0 hr APF is 159 and 72 cells, respectively). As $SMC1^{-/-}$ clones never contain late-born α′/β′ or α/β neurons, we conclude that the reduced clone size is caused by a neuroblast-proliferation defect.

Several additional lines of evidence indicate that mutation of *SMC1* causes axon pruning and neuroblast-proliferation phenotypes: (1) precise excision of the *piggyBac* mutator reversed lethality and all mutant phenotypes (data not shown); (2) MB clones homozygous for a small deletion encompassing *SMC1* (Dorsett et al., 2005) phenocopied our *piggyBac* insertion (Figure 3D); and (3) mutant phenotypes were rescued by transgenes expressing WT SMC1 (see below). We thus conclude that *SMC1* is required for MB neuroblast proliferation and for γ neuron axon pruning.

During *piggyBac* screening, we also isolated an insertion in the 5′UTR of *Stromalin* (*SA*, the yeast *Scc3* homolog), another subunit of the cohesin complex (Figure S3A). Our primary screen with a pan-MB reporter (Gal4-OK107) (Figures 2A and 2B) revealed that homozygous $SA^{-/-}$ clones also fail to prune, in addition to exhibiting a variable neuroblast-proliferation defect (Figures S3B and S3C). This observation suggests that other components of the cohesin complex may also function similarly to SMC1 in regulating axon pruning.

SMC1 Is Required in Postmitotic Neurons for Axon Pruning

Both *SMC1* and *SA* are subunits of the cohesin complex, whose known cellular role is to maintain the cohesion of duplicated sister chromatids during mitosis and meiosis (reviewed in Nasmyth and Haering, 2005). In the absence of cohesin complex function, cells experience precocious sister-chromatid separation, leading to cell-cycle arrest through the action of the spindle checkpoint (Vass et al., 2003). This cell-cycle arrest may explain the reduced proliferation capacity of $SMC1^{-/-}$ neuroblasts. Perdurance of *SMC1* mRNA and/or protein (see Experimental Procedures) in $SMC1^{-/-}$ neuroblast clones may explain why these neuroblasts can still proliferate to some extent. However, homozygous $SMC1^{-/-}$ clones also exhibit defective axon pruning, a process that occurs in terminally differentiated, nondividing neurons. An important question is, therefore, whether SMC1 is required in dividing neuroblasts (as predicted if its role is solely in sister-chromatid cohesion) or in postmitotic neurons for axon pruning.

To address this question, we constructed transgenic flies expressing WT *SMC1* in a Gal4-dependent manner (*UAS-SMC1::HA*). We crossed these flies to two lines expressing Gal4 at different stages of MB development (Gal4-OK107 and -201Y) (Figures 2A and 2B) and tested whether the $SMC1^{-/-}$ γ neuron phenotype can be rescued by either Gal4 driver. Expression of *UAS-SMC1::HA* with either Gal4 line in WT neurons does not result in any detectable gain-of-function phenotype (data not shown). As expected, driving the expression of *UAS-SMC1::HA* in dividing neuroblasts as well as postmitotic neurons by Gal4-OK107 fully rescued both the neuroblast-proliferation and the axon-pruning phenotypes of $SMC1^{-/-}$ neuroblast clones (compare Figure 4Aa to Figure 4Ba for pruning phenotype and Figure 4Ab to Figure 4Bb for proliferation defect). It is difficult to quantify the cell number in these clones because they are densely packed. However, since all cell types are present in the rescued clone, including the latest-born α/β neurons (see Figure 4Ba), we conclude that the proliferation defect was mostly, if not completely, rescued.

In contrast, driving the expression of *SMC1* only in postmitotic neurons with Gal4-201Y (see Figures 2A and 2B) (Yang et al., 1995; Lee et al., 2000b) could not rescue the neuroblast-proliferation defect (compare the size of clones in Figures 4Cb–4Db; the average clone size is 41.9 ± 2 cells for $SMC1^{-/-}$ [n = 10] and 43.5 ± 1.6 cells for $SMC1^{-/-}$ + *UAS-SMC1::HA* [n = 29]). Remarkably, the axon-pruning defect in $SMC1^{-/-}$ MB γ neurons was rescued by postmitotic expression of SMC1 (compare Figure 4Da to Figure 4Ca; complete rescue in 20/27 clones, one remaining dorsal axon in 7/27 clones). These results indicate that SMC1 is required in MB neuroblasts to regulate proliferation, and in postmitotic MB neurons to regulate axon pruning.

SMC1 Regulates EcR-B1 Expression

In addition to its well-characterized function in sister-chromatid cohesion, the cohesin complex has recently been suggested to regulate gene expression through chromatin remodeling (Rollins et al., 1999; Dorsett et al., 2005; reviewed in Dorsett, 2007). A master gene that regulates developmental axon pruning in the fly is the nuclear steroid hormone receptor ecdysone receptor B1 (EcR-B1). EcR-B1 and its coreceptor Usp respond to a late-larval ecdysone pulse by initiating cascades of gene transcription that regulate *Drosophila* metamorphosis, including axon pruning of MB γ neurons (Figure 5A). *usp* is ubiquitously expressed, whereas the expression of *EcR-B1* is highly regulated.

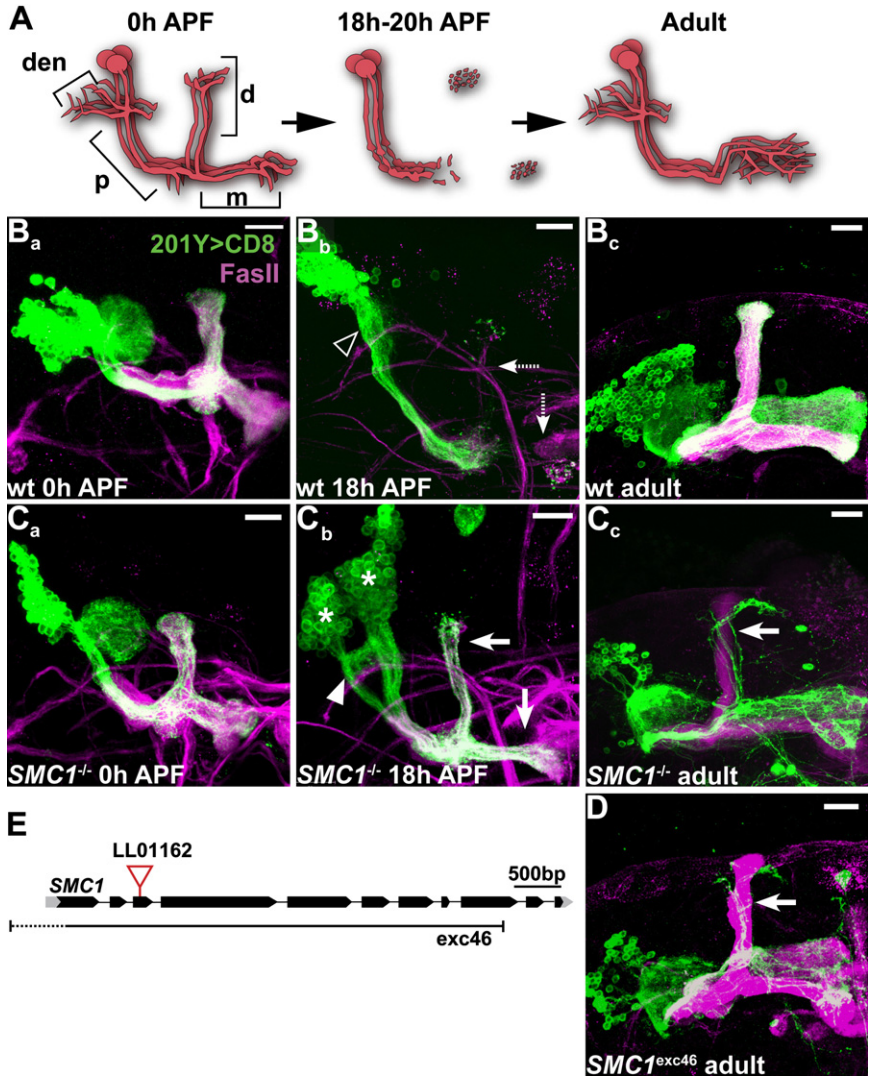

Figure 3. *SMC1* Is Required for Axon Pruning

(A) Scheme of developmental pruning of MB γ neurons. At 0 hr after puparium formation (0h APF), each γ neuron has a single process that gives off dendritic branches (den) near the cell body, continues as an axon peduncle (p), and bifurcates to form a dorsal (d) and a medial (m) branch. The dorsal and medial axon branches, as well as dendrites, are pruned by 18 hr APF, leaving some fragmented axons at the tips of the lobes, but an intact axon peduncle. Later, γ neurons extend axons only to the adult-specific medial lobe, with extensive branches within. Adapted from Watts et al. (2004).

(B–D) (B) WT, (C) $SMC1^{LL01162}$, and (D) $SMC1^{\Delta exc46}$ MB neuroblast MARCM clones labeled with Gal4-201Y. At 0 hr APF, both (Ba) WT and (Ca) $SMC1^{-/-}$ γ neurons project their axons to the dorsal and medial lobes. The cell number within $SMC1^{-/-}$ neuroblast clones is significantly reduced. At 18 hr APF, WT γ neurons have pruned their medial and dorsal axon branches (dashed arrows in [Bb]) as well as their dendrites (open arrowhead). $SMC1^{-/-}$ γ neurons retain most of their axons at this stage (arrows in [Cb]), which persist to adulthood (arrow in [Cc] and [D]). In addition, $SMC1^{-/-}$ γ neurons retain partially unpruned dendrites at 18 hr APF (arrowhead in [Cb]). Asterisks in [Cb] indicate two independent neuroblast clones.

(E) *SMC1* gene structure. *piggyBac* line LL01162 is inserted in the third exon. The approximate borders of the null mutation $SMC1^{\Delta exc46}$ (Scott Page and Scott Hawley, personal communication) are also depicted.

Green, Gal4-201Y-driven mCD8::GFP; magenta, anti-FasII. The scale bars are 20 μm.

EcR-B1 is expressed in MB γ neurons, but is absent from α′/β′ neurons that do not undergo pruning (Lee et al., 2000a). We therefore tested whether expression of EcR-B1 is altered in *SMC1* mutant clones.

We found large differences in EcR-B1 protein levels between WT and mutant clones. In control clones, the vast majority of γ neurons, visualized by Gal4-201Y at 0 hr APF, express high levels of EcR-B1; only 4% of the cells did not express EcR-B1, and 7% express it at reduced levels (Figure 5C; quantified in Figure 5B). By contrast, in $SMC1^{-/-}$ neuroblast clones, the EcR-B1 level is significantly reduced: ~30% of the cells express no EcR-B1, whereas another 20% express low levels (Figure 5D; quantified in Figure 5B).

Since the size of WT and $SMC1^{-/-}$ neuroblast clones differs significantly, we wanted to ascertain that our measurement of EcR-B1-positive cells was not skewed. To this end, we examined EcR-B1 expression in two *piggyBac* insertions in which clone size is also greatly reduced. As quantified in Figure 5B, in both cases (*Top2* and *mats*), all cells expressed EcR-B1. Indeed, EcR-B1-negative cells in WT clones tend to be located closest to the neuroblast, suggesting that they are the youngest γ neurons that have just differentiated and are beginning to express EcR-B1. Since $SMC1^{-/-}$ (or $Top2^{-/-}$ or $mats^{-/-}$) neuroblast clones most likely arrest proliferation before third-instar larvae judging from their small clone size, these young neurons should not be present. Therefore, in $SMC1^{-/-}$ neuroblast clones, non- or low-EcR-B1-expressing cells are likely early born, and their overrepresentation is most likely caused by failure of *EcR-B1* upregulation. Perdurance of *SMC1* mRNA and protein may account for ~50% of $SMC1^{-/-}$ neurons that still express high levels of EcR-B1 (see Experimental Procedures). The regulation of EcR-B1 expression appears to be specific, as four other proteins we examined—Elav, Dac, Usp, and Cut—did not show any change of expression in $SMC1^{-/-}$ compared to WT γ neurons (Figure S4).

Lack of EcR-B1 expression may account for the axon-pruning defect in $SMC1^{-/-}$ neuroblast clones. Indeed, the percentage of EcR-B1-negative cells correlates well with ~20%–30% unpruned axons in $SMC1^{-/-}$ neuroblast clones. To establish a causal relationship, we tested whether changing the dose of endogenous EcR-B1 would affect the pruning defect in $SMC1^{-/-}$

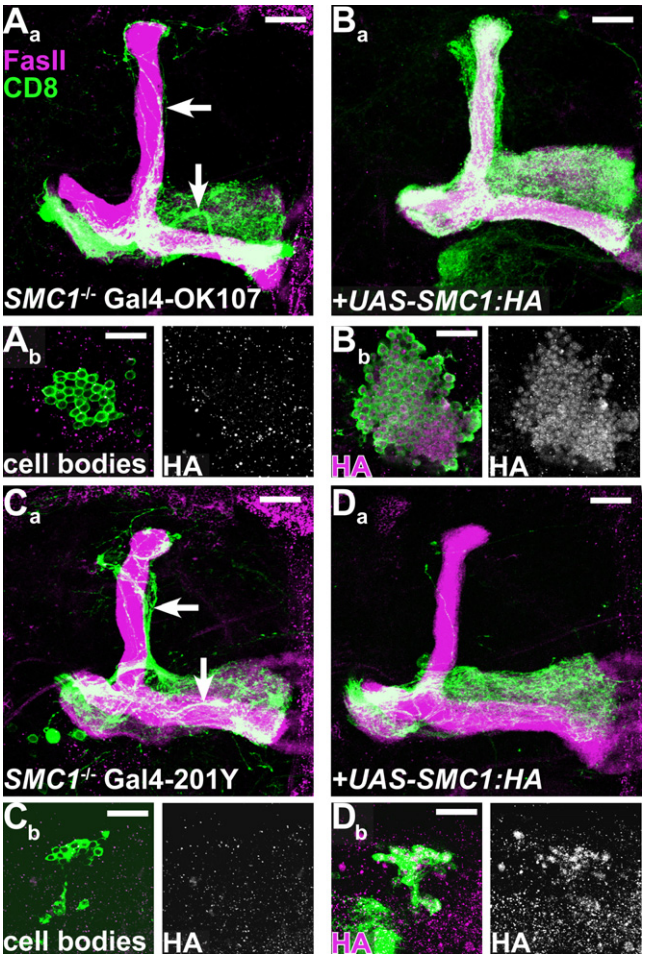

Figure 4. Rescue of Axon-Pruning and Proliferation Defects by *SMC1* Transgene

(A–B) *SMC1*$^{-/-}$ MB neuroblast MARCM clones labeled with Gal4-OK107 exhibit (Aa) unpruned γ neurons (arrows) and (Ab) reduced cell number (also note the lack of α/β or α′/β′ lobes in [Aa]). (B) Expression of the *UAS-SMC1::HA* transgene in mutant clones rescues (Ba and Bb) both phenotypes. (Bb) SMC1-HA protein is predominantly located in the nuclei of neurons (right panel).
(C–D) *SMC1*$^{-/-}$ MB neuroblast MARCM clones labeled with Gal4-201Y exhibit (Ca) unpruned γ neurons (arrows) and (Cb) reduced cell number. (Da) Expression of *UAS-SMC1::HA* only in mutant clones by the postmitotic Gal4 driver (Gal4-201Y) either rescues pruning completely (20/27) or shows only a single unpruned γ neuron (7/27). (Db) The cell number remains unchanged.
Green, (A–B) Gal4-OK107- or (C–D) Gal4-201Y-driven mCD8::GFP; magenta, (Aa–Da) anti-FasII or (Ab–Db) anti-HA. Single confocal sections are shown for (Ab)–(Db). The scale bars are 20 μm.

neuroblast clones. We found that reducing the dosage of *EcR-B1* by generating *SMC1*$^{-/-}$ clones in an *EcR*$^{-/+}$ background resulted in the enhancement of the pruning defects (compare Figure 5H to Figure 5F; quantified in Figure 5E). In addition, *SMC1*$^{-/-}$ clones in a heterozygous background of *babo*, a TGFß receptor that regulates expression of *EcR-B1* (Zheng et al., 2003), also show enhancement of the phenotype, although the clone size is also reduced under this experimental condition (compare Figure 5I to Figure 5F; quantified in Figure 5E). Importantly, overexpression of EcR-B1 markedly suppressed the pruning defects in *SMC1*$^{-/-}$ neuroblast clones (compare Figure 5G to Figure 5F; quantified in Figure 5E). The dosage-sensitive genetic interactions between *SMC1* and *EcR-B1* and, in particular, the suppression of the *SMC1*$^{-/-}$ phenotype by EcR-B1 overexpression strongly suggest that regulation of EcR-B1 expression is a major mechanism by which SMC1 regulates axon pruning. The fact that the suppression is not complete may suggest that either *EcR-B1* is not the only SMC1 target gene in regulating axon pruning or the expression of the *EcR-B1* transgene is not at a sufficient level, or both.

Postmitotic Function of SMC1 in Dendrite Targeting of Olfactory Projection Neurons

SMC1 and *SA* mutants were also independently identified in a parallel screen as affecting olfactory projection neuron (PN) dendrite targeting. In this screen, we used Gal4-GH146, which is expressed in ~90 PNs originating from 3 different neuroblast lineages generating anterodorsal (ad), lateral (l), and ventral (v) PNs (Stocker et al., 1997; Jefferis et al., 2001). PNs are prespecified by lineage and birth order to target their dendrites to specific glomeruli of the antennal lobe and form synapses with incoming olfactory receptor neuron axons (Jefferis et al., 2001).

WT neuroblast clones from all three PN lineages target stereotypic sets of glomeruli (Figures 6A–6C) (Jefferis et al., 2001). *SMC1*$^{-/-}$ PN neuroblast clones have a mild reduction of cell number, likely reflecting proliferation defects similar to those observed in MB neurons. Furthermore, PNs of all three neuroblast lineages show dendrite-targeting defects (Figures 6D–6F). For example, WT adPNs always target to the VA3 glomerulus, whereas 9 out of 12 examined *SMC1*$^{-/-}$ adPNs do not innervate VA3 (dotted outlines in Figures 6A and 6D). The failure to innervate VA3 is not a consequence of proliferation defects, since VA1d PNs are born after VA3 PNs in the adPN lineage (Jefferis et al., 2001), and the VA1d glomerulus is always innervated. The DA1 glomerulus is always innervated by WT lPN neuroblast clones, but it was not innervated by 12 out of 14 *SMC1*$^{-/-}$ neuroblast clones (dotted outlines in Figures 6B and 6E). In both adPNs and lPNs, lineage-inappropriate glomeruli are often innervated (asterisks in Figures 6D and 6E). vPNs show the most dramatic phenotype with regard to dendrite targeting. Dendrites spill outside the antennal lobe with extensive branching into the subesophageal ganglion (SOG) and the lateral side of the antennal lobe (7/7), whereas appropriate target glomeruli (like DA1 and VA1lm) occasionally fail to be innervated (e.g., DA1: 2/7) (Figure 6F). Dendrites and axons of *SMC1*$^{-/-}$ single-cell clones target correctly (data not shown), likely due to perdurance of SMC1 WT protein. Most axons of *SMC1*$^{-/-}$ PNs branch and terminate normally in higher brain centers (data not shown); however, we cannot exclude a role of SMC1 in axon targeting due to the lack of resolution in neuroblast clones.

To distinguish whether the dendrite-targeting defects are caused by the requirement of SMC1 in neuroblasts or postmitotic neurons, we performed rescue experiments by driving the expression of a *UAS-SMC1::HA* transgene with Gal4-GH146, which is expressed in postmitotic PNs, but not in the neuroblast (Spletter et al., 2007). As expected, postmitotic expression of SMC1 does not rescue the reduction of cell number in all three types of neuroblast clones. Targeting of later-born PNs is not restored since these PNs may never have been born (e.g., DM6). Nevertheless, we observe a significant rescue of dendrite-targeting

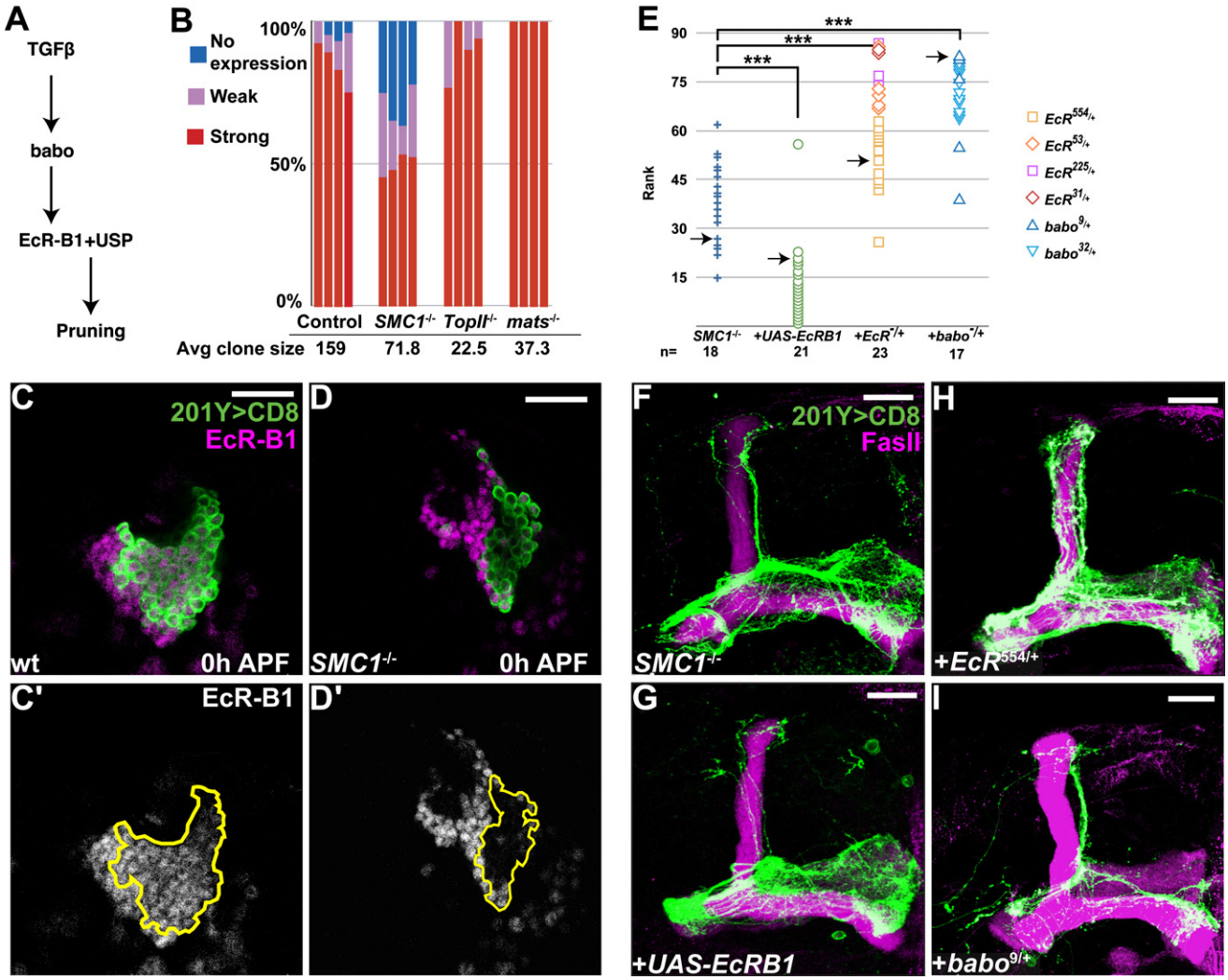

Figure 5. *SMC1* Affects Pruning by Regulating the Levels of EcR-B1

(A) Scheme of the TGFβ/EcR-B1 pathway regulating MB axon pruning.

(B) Summary of EcR-B1 expression in MB neuroblasts at 0 hr APF. Four neuroblast clones for each genotype were blindly analyzed; cells were classified as expressing high, low, or no EcR-B1. The average clone size is also shown.

(C and D) Expression of EcR-B1 (magenta in [C] and [D]; white in [C′] and [D′]) in (C) WT and (D) $SMC1^{-/-}$ MB neuroblast clones. The extent of the clone is depicted in (C′) and (D′) by a yellow line. Single confocal sections are shown.

(E) Summary of genetic interactions. To analyze the suppression or enhancement of the $SMC1^{-/-}$ pruning phenotype, 79 confocal Z projections from different genotypes were blindly ranked for the severity of the pruning defect. The severity was determined by comparing the unpruned dorsal γ axons to pruned γ axons in the adult-specific medial lobe; these pruned axons can be distinguished from unpruned medial axons, as they branch extensively and are located at a more dorsal and posterior position. The ranks grouped by genotypes are shown. Symbols for different *EcR* and *baboon* alleles are shown on the right. Pairwise Mann-Whitney U tests were performed to determine significance: ***, $p < 0.001$. Arrows indicate the examples shown in (F)–(I).

(F–I) Genetic interactions between *SMC1* and *EcR-B1*. (F) $SMC1^{-/-}$ MB neuroblast clone with additional expression of *UAS-EcR-B1* in (G) mutant clone, in (H) an *EcR* heterozygous background, and in a (I) *babo* heterozygous background.

Green represents Gal4-201Y-driven mCD8::GFP, and magenta is (C and D) anti-EcR-B1 or (F–I) anti-FasII. The scale bars are 20 μm.

defects in all three PN lineages (Figures 6G–6I). In $SMC1^{-/-}$ neuroblast clones expressing SMC1::HA, adPNs always target to VA3 (7/7) (Figure 6G, dotted outline), lPNs always target to DA1 (6/6) (Figure 6H, dotted outline), and vPNs are either rescued to a complete WT innervation pattern (3/5) or show minor dendritic misrouting to the SOG (2/5) (Figure 6I, arrow), with DA1 being targeted in all examined brain hemispheres (5/5). Thus, postmitotic expression of *SMC1* is sufficient to rescue PN dendrite-targeting defects.

A *piggyBac* insertion in another cohesin subunit, *SA*, causes similar, though less severe, PN dendrite defects: 6/15 $SA^{-/-}$ adPN neuroblast clones fail to target VA3, and 2/18 $SA^{-/-}$ lPN neuroblast clones fail to innervate DA1. All neuroblast clones spill into additional glomeruli in medial and dorsal areas of the antennal lobe (Figures S3D–S3F). Dendrites of vPNs are often misrouted to the SOG (3/8; data not shown).

The mistargeting phenotype of $SMC1^{-/-}$ or $SA^{-/-}$ PNs resembles the phenotype reported for $cut^{-/-}$ PNs (Komiyama and Luo,

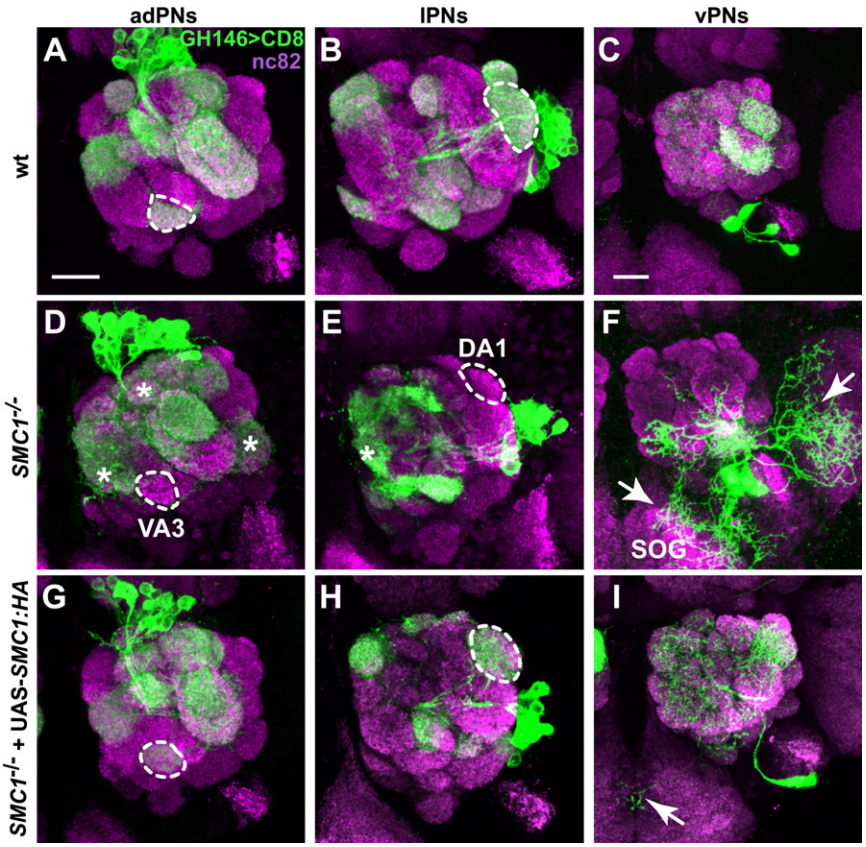

Figure 6. *SMC1* Is Required for PN Dendrite Targeting

(A–C) Stereotypic dendrite projection pattern of WT neuroblast clones that give rise to (A) adPNs, (B) lPNs, and (C) vPNs.

(D–F) $SMC1^{-/-}$ PNs exhibit dendrite-targeting defects. (D) $SMC1^{-/-}$ adPNs do not innervate VA3 (9/12; dotted outline), but instead project to several inappropriate glomeruli in the medial and dorsal parts of the antennal lobe and VL2a (asterisks). (E) $SMC1^{-/-}$ lPNs fail to target DA1 (12/14; dotted outline) but innervate additional medial glomeruli (asterisk). (F) $SMC1^{-/-}$ vPNs show the most severe targeting defects, with large portions of dendrites targeting to the SOG and lateral areas outside the antennal lobe (arrows).

(G–I) Postmitotic expression of SMC1::HA in $SMC1^{-/-}$ PNs fully rescues dendrite targeting in (G) adPNs and (H) lPNs. vPN dendrites are either indistinguishable from WT or show (I) rare dendrites wandering to the SOG (arrow).

Dotted outlines represent selected glomeruli used for scoring the penetrance of *SMC1* mutant phenotypes and corresponding rescues: VA3 for adPNs (in [A], [D], and [G]), DA1 for lPNs (in [B], [E], and [H]). Magenta, nc82 as a presynaptic marker for all glomeruli; green, *UAS-mCD8::GFP* driven by Gal4-GH146. The scale bars are 20 μm.

2007). As it was previously shown that SMC1 regulates the expression of *cut* in the developing wing (Dorsett et al., 2005), and Cut is expressed in a subset of PNs (Komiyama and Luo, 2007), we tested whether Cut expression is regulated by SMC1 in PNs. However, we did not find any change in the Cut protein level in $SMC1^{-/-}$ clones (Figures S4D and S4E), nor when *UAS-SMC1::HA* was expressed in PNs (data not shown).

In summary, mutations in two cohesin subunits, *SA* and *SMC1*, lead to similar defects in MB axon pruning as well as similar defects in PN dendrite targeting. Rescue of the SMC1 defects by using *UAS-SMC1* driven by two different postmitotic Gal4 lines strongly suggests that cohesin regulates diverse aspects of morphogenesis in postmitotic neurons.

DISCUSSION

piggyBac Insertional Mutagenesis for Mosaic Screening

Forward genetic screens in mosaic animals are a powerful method for systematically identifying genes that are required for complex biological processes occurring late in development. In this study, we modified existing *piggyBac* tools to be more mutagenic and compatible with mosaic screening.

Previous studies showed that although 80% of *piggyBac* insertions fall within genes, mutagenicity is decreased by its preferential targeting to introns (Hacker et al., 2003; Bellen et al., 2004). To increase the mutagenicity of intronic insertions, we added to the *piggyBac* mutator splice acceptors followed by stop codons in all three frames in both orientations. Indeed, the proportion of lethal mutations is significantly higher compared to previous reports, and our intronic insertions are almost as mutagenic as insertions in the 5′UTR and CDS. According to the postulation that about one-third of fly genes are essential for viability (Miklos and Rubin, 1996), our percentage of lethal mutations (~28%) is approaching the highest possible mutagenicity with insertional mutagenesis.

Insertional mutagenesis screens are time consuming at the front end of generating mutants. To optimize the efficiency of the screen, we developed protocols to obtain the insertion data at the earliest step possible. This allowed ~30% of the insertions (intergenic plus unmapped insertions due to repetitive or short sequence) to be discarded before stock establishment. In addition, knowledge of the insertion site enabled us to use MARCM-ready flies with the appropriate FRT for mosaic screening. Although generating mutants is more time consuming and costly than EMS mutagenesis, the ease of mapping compensates for the additional effort. Knowledge of both the phenotype and gene identity enables experimenters to make well-informed decisions as to which mutants to pursue further. Moreover, the large collection of molecularly defined *piggyBac* insertions described here should be useful to researchers conducting additional mosaic screens or candidate mutant analyses.

Postmitotic Neuronal Functions of the Cohesin Complex

Developmental axon pruning of MB γ neurons is a complex process that incorporates cell specificity, spatial restrictions, and temporal precision. We identified two subunits of the cohesin complex as essential for pruning. $SMC1^{-/-}$ neuroblast clones also revealed a clear defect in neuroblast proliferation. This

provides in vivo support to previous studies showing that precocious sister-chromatid separation leads to cell-cycle arrest, most likely by triggering the spindle checkpoint mechanism (Vass et al., 2003). A second phenotype in *SMC1*$^{-/-}$ neuroblast clones is that the postmitotic progeny exhibit a defect in developmental axon pruning.

A possible explanation of the role of *SMC1* in axon pruning is that the pruning defect is an indirect consequence of precocious sister-chromatid separation. We ruled out this hypothesis by showing that postmitotic expression of SMC1 is sufficient to rescue the pruning phenotype, thus uncovering a novel function for SMC1 in postmitotic neurons. By contrast, the neuroblast-proliferation defect could only be rescued when SMC1 was expressed in the dividing neuroblast.

A more mechanistic understanding of the effects of SMC1 comes with the observation that there is a significant reduction of EcR-B1 protein levels in *SMC1*$^{-/-}$ neuroblast clones of MB γ neurons. In addition, reducing levels of EcR, or the TGF-β receptor Baboon, which is essential for EcR-B1 upregulation, enhances the pruning defect of *SMC1*$^{-/-}$ neuroblast clones. Moreover, forced expression of EcR-B1 in *SMC1*$^{-/-}$ neuroblast clones partially suppresses axon-pruning defects. Since EcR-B1 is a major regulator of MB axon pruning (Lee et al., 2000a), it is likely that regulation of its levels accounts for the function of SMC in axon pruning. Although our study does not establish how SMC1 regulates EcR-B1, a recent study shows that the cohesin complex binds to the *EcR* locus (Misulovin et al., 2007), strongly suggesting a direct regulation at the transcriptional level.

The mechanism of gene regulation by SMC1 is not well understood. It therefore remains unclear whether SMC1 has a separate function unrelated to its participation in the cohesin complex, or if part or the entire cohesin machinery is utilized for postmitotic gene regulation. Our data support the latter hypothesis. We find that a regulatory subunit of cohesin, SA, which does not directly bind SMC1, is also essential for axon pruning. In addition, Pauli et al. (2008) (this issue of *Developmental Cell*) show that postmitotic inactivation of another cohesin subunit, Rad21, in MB γ neurons also leads to a pruning defect. We therefore suggest that SMC1 acts to regulate gene expression as part of the cohesin complex that includes SA.

Our study also suggests that the cohesin complex regulates diverse morphogenesis aspects of postmitotic neurons. We show that both SMC1 and SA are essential for correct dendrite targeting of PNs. Postmitotic expression of WT SMC1 rescues dendrite-targeting defects of *SMC1* mutant clones. We postulate that cohesin has additional functions in postmitotic neurons, as inactivation of the cohesin complex in all postmitotic neurons results in lethality (Pauli et al., 2008). As complete ablation of the MB (de Belle and Heisenberg, 1994) or large subsets of PNs (Berdnik et al., 2006) does not result in lethality, cohesin must also be necessary in other postmitotic neurons. Interestingly, the *C. elegans Scc4* homolog, *Mau-2*, which is part of the cohesin loading complex, is involved in neuronal migration (Takagi et al., 1997; Seitan et al., 2006), again suggesting that cohesin has a wide role in neuronal morphogenesis.

Previous studies have suggested that cohesin inhibits the expression of Cut in the dividing wing disc by interfering with the communication between a distant enhancer and the promoter (Dorsett, 2007). We show that, in postmitotic MB neurons, SMC1 positively regulates EcR-B1 levels. However, we did not observe any change in Cut levels, evidenced by both loss-of-function or overexpression of SMC1 in MB γ neurons or PNs. These observations suggest that cohesin regulates different genes in different developmental contexts.

Mutations in several cohesin subunits, such as *Smc1a* and *Smc3*, or proteins necessary for its function, such as *NIPBL*, a homolog of *Nipped-B*/*Scc2*, are causal genes of a rare disorder called Cornelia de Lange Syndrome (CdLS) (Strachan, 2005; Musio et al., 2006; Deardorff et al., 2007). CdLS patients exhibit multiple physical and neurodevelopmental deficits. Patients with mutations in *Smc1a* exhibit mild forms of the syndrome, but a mild-to-moderate mental retardation is the most penetrant symptom for these patients. Our finding raises the possibility that, in addition to chromatid cohesion, defective SMC1 function in postmitotic neurons may contribute to the neurodevelopmental and mental deficits of CdLS patients.

EXPERIMENTAL PROCEDURES

piggyBac Vector and Mutant Generation

The *piggyBac* mutator pXL-BacII-SAstopDsRed was generated by cloning an EcoRI-EcoRV fragment that we created (Genbank accession code: EU257621) into EcoRI-EcoRV-restricted pXL-BacII-ECFP (Li et al., 2005). Germline transformation was performed by using routine methods by coinjecting the *piggyBac* transposase-encoding plasmid phspBac (a gift from A. Handler). The genetic scheme for generating mutants is presented in the Supplemental Experimental Procedures. Flies containing *piggyBac* transposase were described previously (Hacker et al., 2003). Insertion sites were obtained by performing inverse PCR by following a protocol presented in the Supplemental Experimental Procedures. Sequencing and alignments were done by Quintara (http://www.quintarabio.com/).

Mosaic Analyses, Fly Stocks, and Transgene Construction

Mosaic analyses with MARCM to generate MB and PN neuroblast clones were performed as previously described (Lee et al., 2000a; Wu and Luo, 2006) by using Gal4-201Y, -OK107, and -GH146. An intrinsic feature of mosaic analysis with MARCM is that from the moment a clone is generated, no new functional mRNA or protein is made in mutant cells. Nevertheless, preexisting mRNAs and proteins inherited from heterozygous parental cells can persist and function normally for a certain period of time, resulting in perdurance.

To generate *UAS-SMC1*, cDNA containing the whole coding region was amplified by using the following primers (5′-3′): CACCATGACCGAAGAGGAC GAC and CGTGTCCTCGAACGTTGTCAAGTC. The product was subcloned into pENTR-D/TOPO (Invitrogen) and then recombined into pTWH (Gateway Collection, *Drosophila* Genomics Resource Center, Bloomington, IN) by using Gateway LR clonase II enzyme mix (Invitrogen). *UAS-EcR-B1* was described previously (Lee et al., 2000a); to obtain a second chromosome insertion, we mobilized the transgene by routine P-element transposition. The *SMC1*$^{\Delta exc46}$ fly was obtained from S. Page and S. Hawley. All other alleles used in this manuscript were obtained from the Bloomington Stock Center.

Immunostaining

Fly brains were dissected, fixed, and processed for whole-mount immunostaining as previously described (Lee et al., 1999; Lee and Luo, 1999). Conditions for primary antibodies are given in the Supplemental Experimental Procedures.

RT-PCR

For semiquantitative RT-PCR, cDNA equivalent to ~1–0.5 ng RNA was used for amplification at 64°C for 27 cycles by using phusion taq (Finnzymes, Espoo, Finland). For α-tubulin and β-actin controls, a sample diluted by a factor of 4 was used. Primer sequences can be obtained upon request.

Supplemental Data

Supplemental Data include four figures, two tables, Supplemental Experimental Procedures, and Supplemental References and are available at http://www.developmentalcell.com/cgi/content/full/14/2/227/DC1/.

ACKNOWLEDGMENTS

We thank U. Hacker, D. Dorsett, A. Handler, S. Page, S. Howley, E. Buchner, R. Barrio, and the Bloomington Stock Center for reagents; K. Nasmyth and A. Pauli for sharing unpublished data and for comments and discussion; T. Clandinin, M. Schuldiner, and members of the L.L. lab, especially E. Hoopfer and B. Tasic, for comments and discussion; and C. Guo, N. Woodling, W. Hong, and A. Fan for assistance. This work was supported by fellowships from the European Molecular Biology Organization (O.S.), the Human Frontier Science Program (D.B.), and National Institutes of Health grant R37-NS041044 (L.L.). L.L. is a Howard Hughes Medical Institute investigator.

Received: August 13, 2007
Revised: October 24, 2007
Accepted: November 2, 2007
Published: February 11, 2008

REFERENCES

Awasaki, T., and Ito, K. (2004). Engulfing action of glial cells is required for programmed axon pruning during *Drosophila* metamorphosis. Curr. Biol. *14*, 668–677.

Bellen, H.J., Levis, R.W., Liao, G., He, Y., Carlson, J.W., Tsang, G., Evans-Holm, M., Hiesinger, P.R., Schulze, K.L., Rubin, G.M., et al. (2004). The BDGP gene disruption project: single transposon insertions associated with 40% of *Drosophila* genes. Genetics *167*, 761–781.

Berdnik, D., Chihara, T., Couto, A., and Luo, L. (2006). Wiring stability of the adult *Drosophila* olfactory circuit after lesion. J. Neurosci. *26*, 3367–3376.

Bishop, D.L., Misgeld, T., Walsh, M.K., Gan, W.B., and Lichtman, J.W. (2004). Axon branch removal at developing synapses by axosome shedding. Neuron *44*, 651–661.

Celniker, S.E., Wheeler, D.A., Kronmiller, B., Carlson, J.W., Halpern, A., Patel, S., Adams, M., Champe, M., Dugan, S.P., Frise, E., et al. (2002). Finishing a whole-genome shotgun: release 3 of the *Drosophila melanogaster* euchromatic genome sequence. Genome Biol. *3*, RESEARCH0079.

Ciosk, R., Shirayama, M., Shevchenko, A., Tanaka, T., Toth, A., Shevchenko, A., and Nasmyth, K. (2000). Cohesin's binding to chromosomes depends on a separate complex consisting of Scc2 and Scc4 proteins. Mol. Cell *5*, 243–254.

Crittenden, J.R., Sloulakis, E.M.C., Han, K.-A., Kalderon, D., and Davis, R.L. (1998). Tripartite mushroom body architecture revealed by antigenic markers. Learn. Mem. *5*, 38–51.

de Belle, J.S., and Heisenberg, M. (1994). Associative Odor learning in *Drosophila* abolished by chemical ablation of mushroom bodies. Science *263*, 692–695.

Deardorff, M.A., Kaur, M., Yaeger, D., Rampuria, A., Korolev, S., Pie, J., Gil-Rodriguez, C., Arnedo, M., Loeys, B., Kline, A.D., et al. (2007). Mutations in cohesin complex members SMC3 and SMC1A cause a mild variant of cornelia de Lange syndrome with predominant mental retardation. Am. J. Hum. Genet. *80*, 485–494.

Dorsett, D. (2007). Roles of the sister chromatid cohesion apparatus in gene expression, development, and human syndromes. Chromosoma *116*, 1–13.

Dorsett, D., Eissenberg, J.C., Misulovin, Z., Martens, A., Redding, B., and McKim, K. (2005). Effects of sister chromatid cohesion proteins on cut gene expression during wing development in *Drosophila*. Development *132*, 4743–4753.

Gruber, S., Haering, C.H., and Nasmyth, K. (2003). Chromosomal cohesin forms a ring. Cell *112*, 765–777.

Hacker, U., Nystedt, S., Barmchi, M.P., Horn, C., and Wimmer, E.A. (2003). piggyBac-based insertional mutagenesis in the presence of stably integrated P elements in *Drosophila*. Proc. Natl. Acad. Sci. USA *100*, 7720–7725.

Hirano, T. (2006). At the heart of the chromosome: SMC proteins in action. Nat. Rev. Mol. Cell Biol. *7*, 311–322.

Hoopfer, E.D., McLaughlin, T., Watts, R.J., Schuldiner, O., O'Leary, D.D., and Luo, L. (2006). Wlds protection distinguishes axon degeneration following injury from naturally occurring developmental pruning. Neuron *50*, 883–895.

Horn, C., Jaunich, B., and Wimmer, E.A. (2000). Highly sensitive, fluorescent transformation marker for *Drosophila* transgenesis. Dev. Genes Evol. *210*, 623–629.

Huang, C.E., Milutinovich, M., and Koshland, D. (2005). Rings, bracelet or snaps: fashionable alternatives for Smc complexes. Philos. Trans. R. Soc. Lond. B Biol. Sci. *360*, 537–542.

Ito, K., Awano, W., Suzuki, K., Hiromi, Y., and Yamamoto, D. (1997). The *Drosophila* mushroom body is a quadruple structure of clonal units each of which contains a virtually identical set of neurons and glial cells. Development *124*, 761–771.

Jager, H., Herzig, A., Lehner, C.F., and Heidmann, S. (2001). *Drosophila* separase is required for sister chromatid separation and binds to PIM and THR. Genes Dev. *15*, 2572–2584.

Jefferis, G.S., Marin, E.C., Stocker, R.F., and Luo, L. (2001). Target neuron prespecification in the olfactory map of *Drosophila*. Nature *414*, 204–208.

Komiyama, T., and Luo, L. (2007). Intrinsic control of precise dendritic targeting by an ensemble of transcription factors. Curr. Biol. *17*, 278–285.

Kuo, C.T., Jan, L.Y., and Jan, Y.N. (2005). Dendrite-specific remodeling of *Drosophila* sensory neurons requires matrix metalloproteases, ubiquitin-proteasome, and ecdysone signaling. Proc. Natl. Acad. Sci. USA *102*, 15230–15235.

Lee, T., and Luo, L. (1999). Mosaic analysis with a repressible cell marker for studies of gene function in neuronal morphogenesis. Neuron *22*, 451–461.

Lee, T., Lee, A., and Luo, L. (1999). Development of the *Drosophila* mushroom bodies: sequential generation of three distinct types of neurons from a neuroblast. Development *126*, 4065–4076.

Lee, T., Marticke, S., Sung, C., Robinow, S., and Luo, L. (2000a). Cell-autonomous requirement of the USP/EcR-B ecdysone receptor for mushroom body neuronal remodeling in *Drosophila*. Neuron *28*, 807–818.

Lee, T., Winter, C., Marticke, S.S., Lee, A., and Luo, L. (2000b). Essential roles of *Drosophila* RhoA in the regulation of neuroblast proliferation and dendritic but not axonal morphogenesis. Neuron *25*, 307–316.

Li, X., Harrell, R.A., Handler, A.M., Beam, T., Hennessy, K., and Fraser, M.J., Jr. (2005). piggyBac internal sequences are necessary for efficient transformation of target genomes. Insect Mol. Biol. *14*, 17–30.

Liao, G.C., Rehm, E.J., and Rubin, G.M. (2000). Insertion site preferences of the P transposable element in *Drosophila melanogaster*. Proc. Natl. Acad. Sci. USA *97*, 3347–3351.

Liu, X.B., Low, L.K., Jones, E.G., and Cheng, H.J. (2005). Stereotyped axon pruning via plexin signaling is associated with synaptic complex elimination in the hippocampus. J. Neurosci. *25*, 9124–9134.

Losada, A., and Hirano, T. (2005). Dynamic molecular linkers of the genome: the first decade of SMC proteins. Genes Dev. *19*, 1269–1287.

Luo, L., and O'Leary, D.D. (2005). Axon retraction and degeneration in development and disease. Annu. Rev. Neurosci. *28*, 127–156.

Marin, E.C., Watts, R.J., Tanaka, N.K., Ito, K., and Luo, L. (2005). Developmentally programmed remodeling of the *Drosophila* olfactory circuit. Development *132*, 725–737.

Miklos, G.L., and Rubin, G.M. (1996). The role of the genome project in determining gene function: insights from model organisms. Cell *86*, 521–529.

Misulovin, Z., Schwartz, Y.B., Li, X., Kahn, T.G., Gause, M., MacArthur, S., Fay, J.C., Eisen, M.B., Pirrotta, V., Biggin, M.D., et al. (2007). Association of cohesin and Nipped-B with transcriptionally active regions of the *Drosophila melanogaster* genome. Chromosoma in press. Published online October 27, 2007. 10.1007/s00412-007-0129-1.

Musio, A., Selicorni, A., Focarelli, M.L., Gervasini, C., Milani, D., Russo, S., Vezzoni, P., and Larizza, L. (2006). X-linked Cornelia de Lange syndrome owing to SMC1L1 mutations. Nat. Genet. *38*, 528–530.

Nasmyth, K. (2005). How might cohesin hold sister chromatids together? Philos. Trans. R. Soc. Lond. B Biol. Sci. *360*, 483–496.

Nasmyth, K., and Haering, C.H. (2005). The structure and function of SMC and kleisin complexes. Annu. Rev. Biochem. *74*, 595–648.

Newsome, T.P., Asling, B., and Dickson, B.J. (2000a). Analysis of *Drosophila* photoreceptor axon guidance in eye-specific mosaics. Development *127*, 851–860.

Newsome, T.P., Schmidt, S., Dietzl, G., Keleman, K., Asling, B., Debant, A., and Dickson, B.J. (2000b). Trio combines with dock to regulate Pak activity during photoreceptor axon pathfinding in *Drosophila*. Cell *101*, 283–294.

Ng, J., and Luo, L. (2004). Rho GTPases regulate axon growth through convergent and divergent signaling pathways. Neuron *44*, 779–793.

Pauli, A., Althoff, F., Oliveira, R.A., Heidmann, S., Schuldiner, O., Lehner, C.F., Dickson, B.J., and Nasmyth, K. (2008). Cell-type-specific TEV protease cleavage reveals cohesin functions in *Drosophila* neurons. Dev. Cell *14*, this issue, 239–251.

Portera-Cailliau, C., Weimer, R.M., De Paola, V., Caroni, P., and Svoboda, K. (2005). Diverse modes of axon elaboration in the developing neocortex. PLoS Biol. *3*, e272.

Raff, M.C., Whitmore, A.V., and Finn, J.T. (2002). Axonal self-destruction and neurodegeneration. Science *296*, 868–871.

Rollins, R.A., Morcillo, P., and Dorsett, D. (1999). Nipped-B, a *Drosophila* homologue of chromosomal adherins, participates in activation by remote enhancers in the cut and Ultrabithorax genes. Genetics *152*, 577–593.

Schubiger, M., Tomita, S., Sung, C., Robinow, S., and Truman, J.W. (2003). Isoform specific control of gene activity in vivo by the *Drosophila* ecdysone receptor. Mech. Dev. *120*, 909–918.

Seitan, V.C., Banks, P., Laval, S., Majid, N.A., Dorsett, D., Rana, A., Smith, J., Bateman, A., Krpic, S., Hostert, A., et al. (2006). Metazoan Scc4 homologs link sister chromatid cohesion to cell and axon migration guidance. PLoS Biol. *4*, e242.

Sheng, G., Thouvenot, E., Schmucker, D., Wilson, D.S., and Desplan, C. (1997). Direct regulation of rhodopsin 1 by Pax-6/eyeless in *Drosophila*: evidence for a conserved function in photoreceptors. Genes Dev. *11*, 1122–1131.

Spletter, M.L., Liu, J., Liu, J., Su, H., Giniger, E., Komiyama, T., Quake, S., and Luo, L. (2007). Lola regulates *Drosophila* olfactory projection neuron identity and targeting specificity. Neural Develop. *2*, 14.

Stocker, R.F., Heimbeck, G., Gendre, N., and de Belle, J.S. (1997). Neuroblast ablation in *Drosophila* P[GAL4] lines reveals origins of olfactory interneurons. J. Neurobiol. *32*, 443–456.

Strachan, T. (2005). Cornelia de Lange Syndrome and the link between chromosomal function, DNA repair and developmental gene regulation. Curr. Opin. Genet. Dev. *15*, 258–264.

Takagi, S., Benard, C., Pak, J., Livingstone, D., and Hekimi, S. (1997). Cellular and axonal migrations are misguided along both body axes in the maternal-effect mau-2 mutants of *Caenorhabditis elegans*. Development *124*, 5115–5126.

Thibault, S.T., Singer, M.A., Miyazaki, W.Y., Milash, B., Dompe, N.A., Singh, C.M., Buchholz, R., Demsky, M., Fawcett, R., Francis-Lang, H.L., et al. (2004). A complementary transposon tool kit for *Drosophila melanogaster* using P and piggyBac. Nat. Genet. *36*, 283–287.

Uhlmann, F., Wernic, D., Poupart, M.A., Koonin, E.V., and Nasmyth, K. (2000). Cleavage of cohesin by the CD clan protease separin triggers anaphase in yeast. Cell *103*, 375–386.

Vass, S., Cotterill, S., Valdeolmillos, A.M., Barbero, J.L., Lin, E., Warren, W.D., and Heck, M.M. (2003). Depletion of Drad21/Scc1 in *Drosophila* cells leads to instability of the cohesin complex and disruption of mitotic progression. Curr. Biol. *13*, 208–218.

Watts, R.J., Hoopfer, E.D., and Luo, L. (2003). Axon pruning during *Drosophila* metamorphosis: evidence for local degeneration and requirement of the ubiquitin-proteasome system. Neuron *38*, 871–885.

Watts, R.J., Schuldiner, O., Perrino, J., Larsen, C., and Luo, L. (2004). Glia engulf degenerating axons during developmental axon pruning. Curr. Biol. *14*, 678–684.

Williams, D.W., and Truman, J.W. (2005). Cellular mechanisms of dendrite pruning in *Drosophila*: insights from in vivo time-lapse of remodeling dendritic arborizing sensory neurons. Development *132*, 3631–3642.

Wu, J.S., and Luo, L. (2006). A protocol for mosaic analysis with a repressible cell marker (MARCM) in *Drosophila*. Nat. Protoc. *1*, 2583–2589.

Xu, T., and Rubin, G.M. (1993). Analysis of genetic mosaics in developing and adult *Drosophila* tissues. Development *117*, 1223–1237.

Yang, M.Y., Armstrong, J.D., Vilinsky, I., Strausfeld, N.J., and Kaiser, K. (1995). Subdivision of the *Drosophila* mushroom bodies by enhancer-trap expression patterns. Neuron *15*, 45–54.

Zheng, X., Wang, J., Haerry, T.E., Wu, A.Y., Martin, J., O'Connor, M.B., Lee, C.H., and Lee, T. (2003). TGF-β signaling activates steroid hormone receptor expression during neuronal remodeling in the *Drosophila* brain. Cell *112*, 303–315.

Accession Numbers

The GenBank accession number for an EcoRI-EcoRV fragment that we created is EU257621.